Kinetically controlled fast crystallization of $M_{12}L_8$ *poly*-[*n*]-catenanes using the 2,4,6-tris(4-pyridyl)benzene ligand and $ZnCl_2$ in aromatic environment.

Stefano Torresi[†] Antonino Famulari,[†] Javier Martí-Rujas[*†,‖]

Dipartimento di Chimica Materiali e Ingegneria Chimica "Giulio Natta", Politecnico di Milano, Via Luigi Mancinelli 7, 20131 Milan, Italy. E-mail: javier.marti@polimi.it; Center for Nano Science and Technology@Polimi, Istituto Italiano di Tecnologia, Via Pascoli 70/3, 20133 Milano, Italy.

ABSTRACT: Kinetic control in the presence of six aromatic solvents has been successfully applied in the synthesis of a *poly*-[*n*]-catenane composed of interlocked $\mathbf{M_{12}L_8}$ icosahedral nanometric cages (*i.e.*, internal voids of 2500 Å^3). Using the exo-tridentate *tris*-pyridyl benzene ligand and $ZnCl_2$ with appropriate templating molecules, due to good ligand aromatic interactions, the metal-organic cages can be synthesized very fast, homogeneously and in large quantities as microcrystalline materials. Synchrotron single crystal X-ray data (100 K) allowed the resolution of nitrobenzene guest molecules at the internal walls of the $\mathbf{M_{12}L_8}$ nanocages while in the central part of the cages the solvent is highly disordered. The guest release occurs in two steps with the disordered nitrobenzene guests released in the first step (lower temperatures) due to the absence of strong cage-guest interactions. Density Functional Theory calculations provided a rationalization of these outcome and in particular, solid state approaches, showed theoretical evidence of the kinetic nature in the formation of the *poly*-[*n*]-catenane by the analysis of the packing energy in terms of monomeric and dimeric cages.

Introduction

Metal-organic cages self-assembled of metal ions and organic ligands by means of coordination bonds are attracting much attention as they form structures with cavities where guest molecules can be included.[1,2,3,4] Discrete monomeric cages are host-guest systems that can be seen as nanoreactors allowing catalysis[5], molecular separation[6] or unique reactivity[7] within their internal space. Two monomeric cages self-assembled by metal directed coordination bonds can be interlocked by *mechanical bonds* to form a catenane.[8,9] The labile nature of the coordination bond is crucial to understand the formation of the catenanes, as cleavage and formation of coordination bonds are needed to form the supramolecular structure.[9] However, catenation remains difficult to predict because there are many factors controlling the interpenetration process.[8,9] For successful catenation an important role is played by the ligand-ligand and ligand-solvent electrostatic interactions that allows the assembling components to pre-assemble by templating effect by considering enthalpic and entropic effects.

While there are many examples of double interpenetrated cages,[9,10,11,12] reports of infinite interlocked nanocages are still rare.[13] The first infinite array of 1D strand of interlocked large $\mathbf{M_{12}L_8}$ nanocages (*i.e.*, *poly*-[*n*]-catenane) as single crystals was reported by slow self-assembly of 2,4,6-tris(4-pyridyl)pyridine (**pytpy**) and $ZnCl_2$[14] which was followed by the ZnI_2 isostructural material.[15] The formation of the interlocked nanocages is explained by the authors due to the electrostatic nature of the ligand core.[13] The π-π interactions arising from the aromatic central part of the ligand are crucial in the formation of the interlocked nanocages, together with the templating solvent.[14] However, in the ZnI_2 system, if **pytpy** is functionalized with a Cl group, under the same crystallization conditions, a 1D coordination polymer is obtained instead of the $\mathbf{M_{12}L_8}$ nanocages.[15] These results, clearly show that "small" ligand modifications can drastically switch the assembling process.[15] Therefore, one should expect that the same *poly*-[*n*]-catenane is also formed if the aromaticity of the central ring is enhanced by substituting the pyridine by a benzene in **pytpy**.

Here using $ZnCl_2$ and the exo-tridentate *tris*-pyridyl benzene (**TPB**) ligand with a richer electron core than that of **pytpy**, the selective formation of the neutral *poly*-[*n*]-catenate $[(ZnCl_2)_{12}(\mathbf{TPB})_8]_n{\cdot}_9(C_6H_5NO_2)$ (**1**) is reported (Scheme 1). Synchrotron single crystal X-ray data reveals that **1** is constituted of icosahedral interlocked $\mathbf{M_{12}L_8}$ cages with 6 ordered and 3 disordered nitrobenzene guests. While slow crystallization gives a mixture of products including **1** and a coordination polymer, kinetically controlled fast synthesis selectively yields **1** in short times, homogeneously and in large quantities. The kinetically controlled synthesis does not allow the "*error-checking*" process for the cages' locking-unlocking process, yielding the formation of the interlocked nanocages as the only product. **1** can be prepared with six aromatic templating solvents (Scheme 1). TG and powder XRD shows that upon heating **1** to 160 °C, there is partial guest release whilst keeping the $\mathbf{M_{12}L_8}$ cages that can uptake nitrobenzene. **1** changes into an unknown phase upon full guest release *ca*. 210 °C. Solid-state Density Functional Theory (DFT) showed that catenation aided by ligand aromatic-aromatic interactions is favored over isolated monomer units as kinetic products according to the energy values.

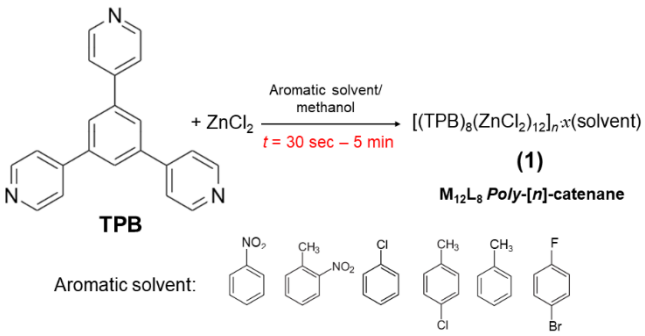

Scheme 1. Ligand **TPB** used in this work self-assembled with $ZnCl_2$ to form a supramolecular $\mathbf{M_{12}L_8}$ nanocage *poly*-[*n*]-catenane with different templating aromatic solvents.

Results and Discussion

Synchrotron Single crystal structure of *poly*-[*n*]-catenane with TPB and $ZnCl_2$. Ligand **TPB** offers the opportunity to explore its coordination chemistry[16] and to be compared to the related MOFs and coordination complexes obtained using other tridentate ligands like the well-known *tris*-(4-pyridyl)-triazine (**TPT**)[17] and **pytpy**. Thus, we started crystallization experiments with **TPB** and $ZnCl_2$ using a slow layering crystallization method (Supporting Information). After *ca*. 5 days block-like (hexagonal habit, Figure 1c) colorless crystals appeared in the walls of the tube mixed with other smaller brownish crystals.[18] A suitable colorless single crystal was mounted in a loop for X-ray crystallographic analysis conducted using synchrotron radiation (Supporting Information).

The $ZnCl_2$ complex crystallizes in the highly symmetric trigonal system in the *R*-3 space group with the following lattice parameters: a = 37.380(10) Å; b = 37.380(10) Å, c = 16.0971(10) Å, V = 19478.6 Å^3; Z = 3.[19] From the X-ray data, the molecular formula is $[(ZnCl_2)_{12}(TPB)_8]_n{\cdot}9(C_6H_5NO_2)$, (from X-ray data n = 6, and TGA n = 9) giving rise to a 0D $\mathbf{M_{12}L_8}$ nanocage (**1**). In the asymmetric unit there are two $ZnCl_2$ units, one TPB ligand, 1/3 of a second ligand and one $C_6H_5NO_2$ guest molecule. Two thirds of the guest molecules have been determined crystallographically while one third remain disordered within the large cavity.

An isolated $\mathbf{M_{12}L_8}$ nanocage can be described as an *icosahedron* (*i.e.*, a Platonic solid) with 8 faces occupied by **TPB** and the remaining triangular 12 faces opened.[20] The open windows have apertures of 22 Å × 13 Å considering the Zn atoms in the opposite sides of the windows (Figure 1). The distance among the two benzene rings in the **TPB** ligands from the top to the bottom of the cage is 20.548 Å. One nitrobenzene guest molecule in the asymmetric unit is ordered and can be resolved by X-ray crystallography. The guest molecule interacts with one **TPB** in the cage due to a good electrostatic interaction among the pyridine group and the electron rich aromatic ring in the nitrobenzene molecule (3.974 Å) (Figure 2). Additionally, one aromatic Zn–Cl···H–$C_{aromatic}$ (2.876 Å; 139°) interaction involving a non-interlacing neighboring $\mathbf{M_{12}L_8}$ nanocage and the nitrobenzene contributes to the ordering of the guest molecules.

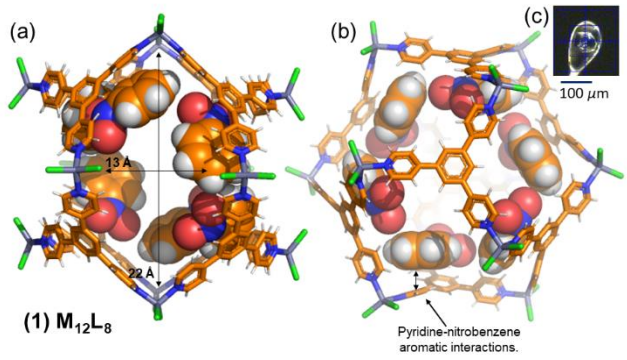

Figure 1. Synchrotron X-ray structure of a discrete $\mathbf{M_{12}L_8}$ nanocage in **1** including the ordered guest molecules. (a) View along one of the openings of the cage. The nanocage has large apertures 22 Å × 13 Å along which the interlocking takes place. (b) View of the nanocage along the [001] crystallographic direction. (c) Single crystal of **1** showing the hexagonal habit.

In the $\mathbf{M_{12}L_8}$ nanocage the ordered solvent molecules are arranged in an hexagonal symmetry while the top and bottom part of the nanocage is free of solvent because it is the area where the nanocages are concatenated (Figure 2b). The central part of the cage is filled with disordered tumbling nitrobenzene molecules not possible to resolve by X-ray data but determined by TGA analysis (see later). The void space occupied by the disordered guests is *ca*. 21 % (*ca*. 4153 Å^3) of the total unit cell volume. The whole metal-organic framework shows no disorder and can be refined with good thermal parameters. The templating effect of large aromatic molecules (*i.e.*, nitrobenzene) seems crucial to maintain the large voids stable even at room temperature.

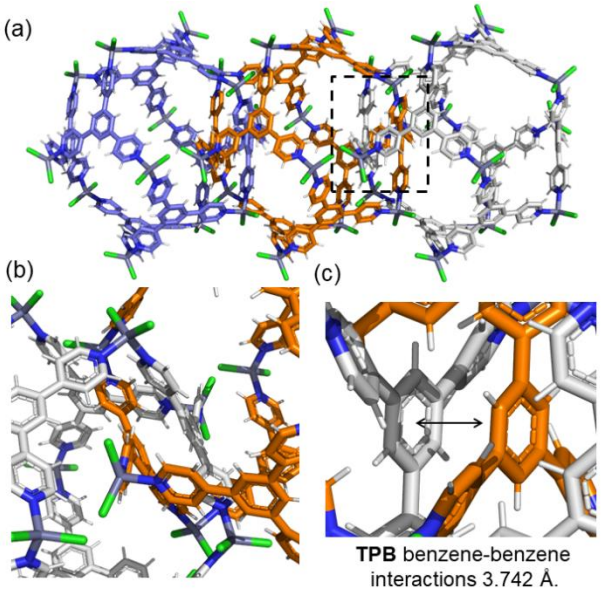

Figure 2. (a) Side-view of three catenated $\mathbf{M_{12}L_8}$ nanocages distinguished by color (blue, orange and white). (b) Zoomed view of two $\mathbf{M_{12}L_8}$ nanocages around the area in which the TPB core benzene-benzene stacking takes place. The electrostatic interactions are highlighted with an arrow (c). Solvent molecules have been omitted for clarity.

The $\mathbf{M_{12}L_8}$ nanocages are not isolated. Each cage is interpenetrated by two adjacent ones via face-to-face aromatic interactions among electron-rich benzene rings (d = 3.742 Å) of

neighboring $\mathbf{M_{12}L_8}$ units (Figure 2b and 2c). Additional interactions among the Cl and the H atoms of surrounding **TPB** ligand contribute to the overall stabilization of the interlaced icosahedral cages. The complex structure can be described as a *poly*-[*n*]-catenane.

The chains of interlocked icosahedral coordination nanocages expand along the [001] crystallographic direction (Figure 3a). Interestingly, the space left in the cages after the interlocking of the neighboring nanocages is *ca*. 39 % (*ca*. 7558 $Å^3$) of the total unit cell volume by virtually removing the solvents.[21] Each nanocage (*i.e.*, three per unit cell) has an internal volume of ≈ 2500 $Å^3$ (Figure 3b). It is important to notice that the volume occupied by the entropically disordered molecules correspond to 55 % of the total void volume which is considerable compared to the 21 % of the 6 ordered guests.

Therefore, **1** can be regarded as a nanocage filled with liquid-like guest molecules highly disordered only in the central part of the cage. It is important to note that in **1** there are no continuous channels but only isolated voids belonging to each nanocage with included solvent (Figure 3). It might have a direct influence in the solid-state stability but also in the dynamic behavior, for instance in the release/inclusion of guest molecules. To the best of our knowledge, this structure is the first reported of *poly*-[*n*]-catenane composed of interlocked $\mathbf{M_{12}L_8}$ cages using the **TPB** ligand and $ZnCl_2$.

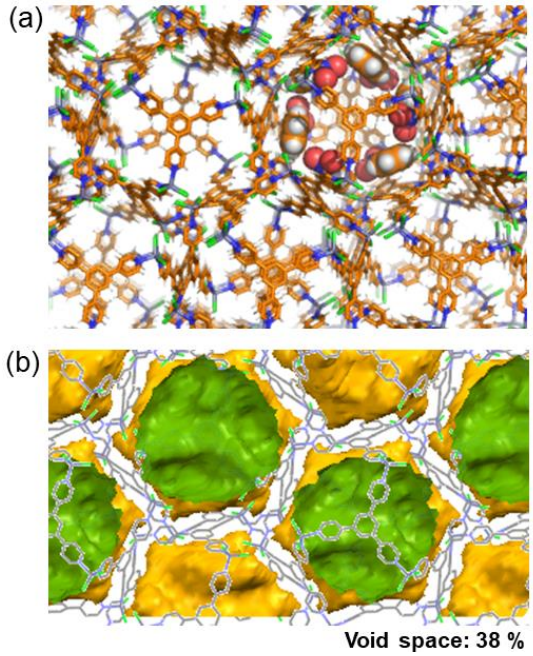

Figure 3. (a) Crystal packing of **1** viewed along the [001] crystallographic direction (*i.e.*, the interlacing direction) with one cage filled with the ordered nitrobenzene molecules (space filling model). (b) Void space shown after removing all the guest molecules in **1**. Green: internal surface; yellow: external surface.

Kinetically controlled synthesis of *poly*-[*n*]-catenane under templating aromatic solvent. An important aspect in the synthesis of this class of materials to study them in the bulk and for their potential industrial applications is the possibility to reproduce selectively the same structure but as microcrystalline materials, homogeneously, in large quantities (multigram scale) and easily in very short times (*i.e.*, 30 secs). However, such selective synthesis has been used in few cases in MOFs[22,23,24] and to the best of our knowledge unknown in *poly*-[*n*]-catenanes. Therefore, a fast crystallization method was used, where ligand **TPB** (120 mg/0.388 mmol) is dissolved in a mixture of nitrobenzene and methanol (14:4 mL). Then a methanolic solution of $ZnCl_2$ (79.33 mg/0.528 mmol in 2 mL of MeOH) was added instantaneously into the vigorously stirring **TPB** solution at room temperature. An immediate microcrystalline white powder precipitated upon the addition of the $ZnCl_2$ (Figure S6). Upon filtration the powder was wet and sticky, therefore it was dried flowing N_2 and left to dry in air for five days. The yield of the reaction is 58 % based on TPB.

Powder XRD analysis of the microcrystalline sample shows that the product was crystalline and revealed that the pattern corresponds to **1** (Figure 4a and 4b). Importantly, the *poly*-[*n*]-catenane structure is formed incredibly fast (*i.e.*, immediately upon $ZnCl_2$ addition), thus it can be considered a *kinetic* product where the mechanical bonds (*i.e.*, catenation) occurs selectively. Compared to charged nanocages, the neutrality of the material allows the *poly*-[*n*]catenation due to good face-to-face aromatic stacking interactions among **TPB** ligands, while the presence of many counterions in ionic cages might difficult poly-catenation due to repulsive forces among charged particles.[13]

Since the role played by the guest molecules is important in the templating effect for the formation of the large $\mathbf{M_{12}L_8}$ nanocages (*i.e.*, entropic contribution), different aromatic and non-aromatic solvents were screened. All the experiments were carried out using the fast crystallization method at room temperature. The additional tested guest molecules that promote the formation of the nanocages are aromatic: nitrotoluene, *p*-chlorotoluene, toluene, chlorobenzene and 1-bromo-4-fluorobenzene. However, if chloroform is used in the fast synthesis the nanocages are not formed (Figure S13). This suggests that most likely large templating molecules are needed for the formation of the nanocages under kinetic control.

The products of each fast synthesis were analyzed by powder XRD analysis by comparing the diffraction pattern with the simulated from single crystal of **1** as depicted in Figure 4. As shown, all the products (Figure 4c-g), correspond to *poly*-[*n*]-catenanes of $\mathbf{M_{12}L_8}$ nanocages. There is a small peak shifting due to small variations in the unit cell depending on the included templating solvent. The changes in the intensities for the two reflections at angles 4.7° and 6.1° in 2θ correspond to the planes with Miller indices (2-10) and (101) respectively, which are affected by disordered solvent such as in the 1-bromo-4-fluorobenzene template (Supporting Information).

In order to check the purity of the crystalline phases, LeBail refinements[25] were carried out for all the microcrystalline products. Because there is a very good agreement in the diffraction patterns from the simulated and experimental powder XRD patterns including nitrobenzene, we used the lattice parameters of **1** as starting unit cell to start out the LeBail refinement. The good fitting of the experimental data corroborates that the microcrystalline product is pure, and no other by-products are obtained (Figure S15). The same procedure was carried out for all the powder XRD patterns obtained by fast synthesis with all the templating guests, also showing pure crystalline phases (Table S1, Supporting Information).

In all the crystallization experiments the products are obtained immediately within 30 seconds and 5 minutes of stirring conditions after the addition of $ZnCl_2$. It is important to highlight that the screening and preparation of the different solvents

can be done within one morning avoiding the time-consuming and difficult growth of single crystals.

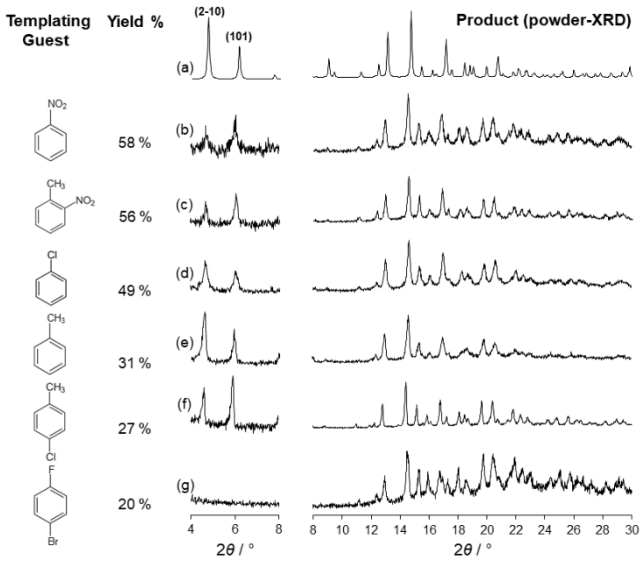

Figure 4. Plot showing the various aromatic molecules tried using the instant synthesis method for the formation of the $\mathbf{M_{12}L_8}$ *poly*-[*n*]-catenanes. For the sake of clarity, the powder XRD patterns are plotted from 4-8 in 2θ ° to show the weak diffraction peaks with Miller indices (2-10) and (101), and from 8 to 30 in 2θ ° the rest of the diffractogram. (a) Simulated powder XRD of **1** (including nitrobenzene (100 K)). Experimental powder XRD patterns obtained with the following solvents (300 K): (b) nitrobenzene; (c) nitrotoluene; (d) chlorotoluene; (e) toluene; (f) *p*-chlorotoluene (g) 1-bromo-4-fluorobenzene.

Thermal stability of microcrystalline *poly*-[*n*]-catenane 1. It is worth to mention the type of interpenetration of the nanocages, which has a direct influence on one of the important features of *poly*-[*n*]-catenanes: the conformational mobility of the cages. While a catenane made of rings can have full rotation, but limited rocking and elongational displacement, in the present case the locking of nanocages results in a restricted rotation and limited elongational and rocking motion.[26] Thus, such constrained mobility of the interlocked nanocages might have a significant role in the dynamic behavior of the overall solid-material. Clearly, such restricted degree of rotation is dictated in part by the opening of the windows where the interlocking takes place.

To quantify the contents in the nanocages thermogravimetrical (TG) analysis was carried out. TG data on the as synthesized powders of **1** (dried with N_2 and left to equilibrate with the atmosphere for 5 days) evidences that the weight loss is *ca*. 35.5 % of the total weight (Figure 5). The TG curve shows that there are two different weight loss events. The first one (from 60 °C-140 °C) corresponds to a *ca*. 12 % of the total weight loss which fits with 3 solvent guest molecules (*i.e.*, disordered ones). The second process (from 140 °C-250 °C), amounting 23 % of the weight loss corresponds to the 6 ordered nitrobenzene guest molecules. The good host-guest interactions result in higher temperatures needed to release the ordered guests in the second thermal event. All the solvent appears to be completely released at 250 °C.

To gain more insights on the dynamic behavior of **1**, a microcrystalline sample was heated in the oven (3h) at 160 °C and monitored its crystallinity by *ex situ* powder X-ray analysis. The diffraction pattern corresponds to the structure of **1** but with significant peak shifting denoting a partial guest release. TG analysis of the heated sample shows that the nanocages still contain guests and the weight loss corresponds to 15.5 % (*i.e.*, 4 nitrobenzene molecules left in the cage). In this case the release of nitrobenzene starts at 150 °C and not at 60 °C as in the synthesized sample (Figure S16), suggesting that the molecules that are being released in the heated sample are tightly bound to the nanocages.

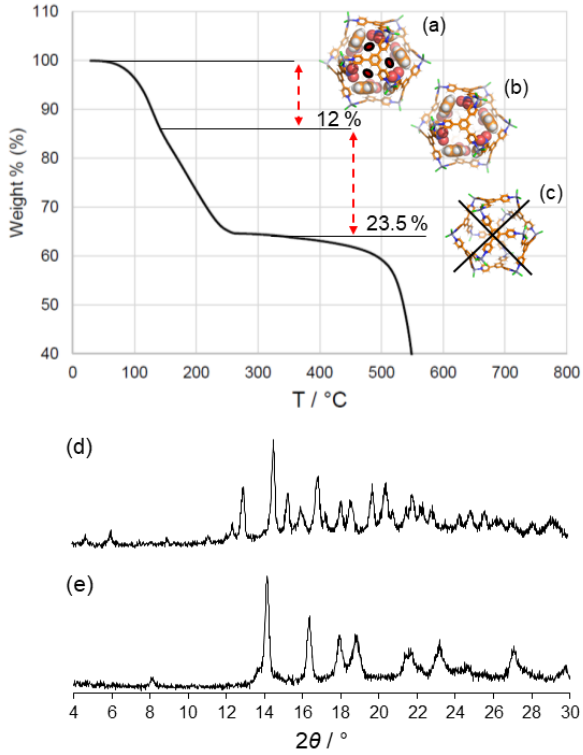

Figure 5. TG experiment of **1**. The first guest release corresponds to the disordered nitrobenzene molecules (weight loss: 12 %) shown as three red dots (a); whereas the second thermal event belongs to the release of the tightly bound ordered molecules (weight loss: 23.5 %) (b). Further heating results in the disruption of **1** and formation of a new phase as corroborated by powder XRD analysis (c). Powder XRD of **1** (d) and the new phase obtained upon heating up to 230 °C (e).

Further, this sample was immersed in nitrobenzene overnight, filtered and dried. From the X-ray data the original structure was re-stablished by comparing the powder XRD patterns the original phase **1** confirming that the $\mathbf{M_{12}L_8}$ nanocages are still formed (Figure S17). However, if **1** is heated up to 230 °C a new phase is formed resulting in a completely different powder diffraction pattern (Figure 5e). This fact is supported from the TG experiment: at 200 °C almost all the guest molecules are released from the cages rendering the structure unstable (Figure 5). Importantly, dipping the new phase obtained at 230 °C in nitrobenzene for two days does not transform into the original structure of **1**, indicating that the structural reorganization is major and the solvent do not reconstruct (*i.e.*, cannot template) the original *poly*-[*n*]-catenanes in **1**. Due to the close packing structure of **1**, in our opinion to allow guest molecules to leave the cages, it must be necessary a distortion on the packing of 1D rods since there is no continuous channel structure.

Density Functional Theory (DFT) solid-state QM calculations. Finally, in order to better understand the stability of the *poly*-[*n*]-catenane **1**, DFT calculations (PBE/DNP level, see Supporting Information), including calculation specific for crystalline solid states, have been carried out. Explicit van der Waals contribution, according to the approach proposed by Grimme.[27] The strategy here adopted showed good results in a number of recent studies of crystalline systems (molecules, polymers and hybrid metal-organic materials).[28,29,30, 31]

As observed experimentally, the structure of **1** is quite stable and forms readily. If we consider the *interaction energies* (E) of the dimers in the structure, we find two kind of "closest" dimers which are both stable. The first dimer unit expands along the crystallographic *c*-axis and is a concatenated structure (*i.e.*, interlocked cages), with an interaction energy *ca.* 150 kcal/mol (Figure 6a). The second dimer unit is a non-concatenated structure (*i.e.*, non-interlocked cages) and has a lower interaction energy of *ca*. 50 kcal/mol (Figure 6a). This variation in the relative *interaction energies* can be understood by the different type of interactions established among the kinetically produced $\mathbf{M_{12}L_8}$ nanocages. In the first studied *dimer* case (*i.e.*, interlocked nanocages) there are very good *benzene-benzene* interactions among the central benzene rings in each concatenated **TPB** ligands (Figure 6a). Such interactions have a strong influence in the formation and stabilization of the *poly*-[*n*]-catenanes (distances among benzene cores *ca*. 3.742 Å) that can be seen also along the [001] crystallographic direction. In the second studied case, without interlocking among the $\mathbf{M_{12}L_8}$ nanocages, the Van der Waals interactions between the cages are less intense as they are short electrostatic contacts. The stabilization energy is *ca*. 1/3 of the energy calculated for the concatenated structure.

The lattice energy (E*) for a *monomer* unit shown in Figure 6b (*i.e.*, the average energy required to extract a single $\mathbf{M_{12}L_8}$ nanocage immersed into the crystalline structure) is very high (436 kcal/mol) compared to a structural unit composed of two interlaced $\mathbf{M_{12}L_8}$ nanocages (*i.e.*, "*dimers*" units; $\mathbf{M_{24}L_{16}}$). If we consider one strand of interlocked $\mathbf{M_{12}L_8}$ nanocages along the crystallographic *c*-axis and calculate the energy required to extract a single infinite chain from the crystalline structure, we obtain a quite high energy (365 kcal/mol) (Figure 6b). This indicates that a simple model of an infinite chain of interlocked $\mathbf{M_{12}L_8}$ nanocages immersed in the structure is a good representation that helps to explain the good stability of **1** easily obtained under *kinetic* control. That is, the rods are very stable and account for most of the lattice energy in the crystal. The weak interactions among the interlocked $\mathbf{M_{12}L_8}$ nanocages (among the 1D chains), are a minimal part of the total energy. With respect to the total lattice energy we miss about 70 kcal/mol that is the average stabilization energy of the spheres in the isolated chain.

Regarding the host-guest interactions it is important to consider the electrostatic potential of the nitrobenzene molecule. The negative region on the nitrobenzene is located at the $-NO_2$ group which interacts with the benzene ring of **TPB** with an energy of *ca.* 34 kcal/mol. Whereas a nitrobenzene molecule at the center of the nanocage has a much lower interaction with the cage is *ca*. 16 kcal/mol which explains its disordered nature in the $\mathbf{M_{12}L_8}$ nanocages.

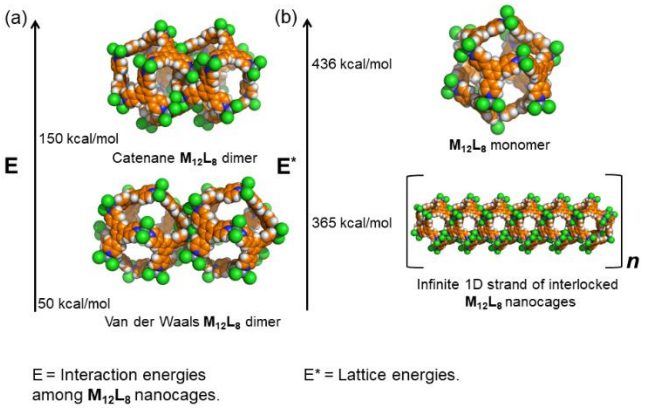

Figure 6. Energy plot showing the relative interaction energies (E) among interlocked and non-interlocked dimers (a); and lattice energies (E*) of a monomer and of an infinite 1D chain of *poly*-[*n*]-catenane (b).

Conclusions

In conclusion we have reported for the first time the high resolution synchrotron X-ray structure of a *poly*-[*n*]-catenane that forms by the interlocking of $\mathbf{M_{12}L_8}$ nanocages having large internal voids filled with partially ordered nitrobenzene. The *poly*-[*n*]-catenane **1** can be selectively crystallized homogeneously under kinetic control by fast crystallization, in large amounts, in short times in the presence of six different aromatic solvents. Thermogravimetric analysis shows that in two events the disordered molecules in the center of the nanocages are released first, while the ordered nitrobenzene needs higher temperatures to be removed. The $\mathbf{M_{12}L_8}$ nanocages in absence of templating solvent collapse into another thermodynamic structure but partially emptied nanocages reabsorb nitrobenzene. Solid-state DFT calculations give insight in the stability of the *poly*-[*n*]-catenane chains and the included solvent molecules. Gaining insights in the formation of [*n*]-catenanes such as the one described herein is important for a better understanding on the factors that contribute to the formation of mechanically interlocked structures. The combination of experimental data and theoretical DFT calculations can be of great help in this understanding. Further work using $ZnBr_2$ and ZnI_2 and **TPB** is being carried out to expand the chemistry of this *poly*-[*n*]-catenanes with the aim of obtaining isostructural materials.

ASSOCIATED CONTENT

Supporting Information includes powder XRD, TG and single crystal X-ray data and DFT calculations details.

AUTHOR INFORMATION

Corresponding Author

*javier.marti@polimi.it

Author Contributions

The manuscript was written through contributions of all authors. All authors have given approval to the final version of the manuscript.

Funding Sources

J. M.-R. thanks Politecnico di Milano for funding (Fondo Chiamata Diretta Internazionalizazzione. Prg. Id. 61566). A. F. acknowledges MIUR for FFARB "Fondo finanziamento delle attività base di ricerca" and CINECA for CPU computational resources.

ACKNOWLEDGMENT

All authors thank the Alba-CELLS Synchrotron, Barcelona for granting with beamtime (BL13-XALOC Macromolceular Crystallography beamline) the Proposal Number 2018092985. The authors thank Dr. Roeland de Boer and Dr. Barbara Machado form the BL13-XALOC beamline for their experimental support. J. M.-R thanks Politecnico di Milano for funding "Fondo Chiamata Diretta Internazionalizazzione. Prg. Id. 61566".

REFERENCES

[1] Seidel, S.R.; Stang, P. J. High-symmetry coordination cages via self-assembly. *Acc. Chem. Res.*, **2002**, *35*, 972-983.

[2] Fujita, M.; Tominaga, M.; Hori, A.; Therrien, B. Coordination assemblies from a Pd(II)-cornered square complex. *Acc. Chem. Res.*, **2005**, *38*, 371-380.

[3] Han, M.; Engelhard, D. M.; Clever, G. H. Self-assembled coordination cages based on banana-shaped ligands. *Chem. Soc. Rev.*, **2014**, *43*, 1848-1860.

[4] Pullen, S.; Clever, G. H. Mixed-ligand Metal−Organic Frameworks and heteroleptic coordination cages as multifunctional scaffolds−A comparison. *Acc. Chem. Res.* **2018**, *51*, 3052−3064.

[5] Yoshizawa, M.; Tamura, M.; Fujita, M. Diels-alder in aqueous molecular hosts: unusual regioselectivity and efficient catalysis. *Science*, **2006**, *312*, 251-254.

[6] Jiménez, A.; Bilbeisi, R. A.; Ronson, T. K.; Zarra, S. Woodhead, C.; Nitschke, J. R. Selective encapsulation and sequential release of guests within a self-sorting mixture of three tetrahedral cages. *Angew. Chem. Int. Ed*. **2014**, *53*, 4556–4560.

[7] Klostermann, J. K.; Yoshizawa, M.; Fujita, M. Functional molecular flasks: new properties and reactions within discrete, self-assembled hosts. *Ang. Chem. Int. Ed.* **2009**, *48*, 3418-3438.

[8] Stoddart, J. F. The mechanical bond. *Chem. Soc. Rev*., **2009**, *38*, 1802–1820.

[9] Frank, M.; Johnstone, M. D.; Clever, G. H. Interpenetrated cage structures. *Chem. Eur. J.* **2016**, *22*, 14104-14125.

[10] Fujita, M.; Fujita, N.; Ogura, K.; Yamaguchi, K. Spontaneous assembly of ten components into two interlocked, identical coordination cages. *Nature* **1999**, *400*, 52-55.

[11] Westcott, A.; Fisher, J.; Harding, L. P.; Rizkallah, P.; Hardie, M. J. Self-assembly of a 3-D triply interlocked chiral [2]catenane. *J. Am. Chem. Soc*., **2008**, *130*, 2950.

[12] Bloch, W. M.; Holstein, J. J.; Dittrich, B.; Hiller, W.; Clever, G. H. Hierarchical assembly of an interlocked M_8L_{16} container. *Angew. Chem. Int. Ed*. **2018**, *57*, 5534–5538.

[13] Kuang, X.; Wu, X.; Yu, R.; Donahue, J. P.; Huang, J.; Lu, C.-Z. Assembly of a metal–organic framework by sextuple intercatenation of discrete adamantane-like cages. *Nat. Chem.* **2010**, *2*, 461.

[14] Heine, J.; auf der Gunne, J. S.; Dehnen, S. Formation of a strandlike polycatenane of icosahedral cages for reversible one-dimensional encapsulation of guests. *J. Am. Chem. Soc.*, **2011**, *133*, 10018-10021.

[15] Constable, E. C.; Zhang, G; Housecroft, C. E.; Zampese, J. A.; Zinc(II) coordination polymers, metallohexacycles and metallocapsules-do we understand self-assembly in metallosupramolecular chemistry: algorithms or serendipity? *CrystEngComm.*, **2011**, *13*, 6864-6870.

[16] The coordination chemistry of **TPB** has never been used in the formation of *poly*-[*n*]-catenanes and is scarcerly used coordination polymers despite its great potential as building block in MOF chemistry. For an example of a MOF with **TPB**: Shao, F.; Li, J.; Tong, J.P.; Zhang, J.; Chen, M. G.; Zheng, Z.; Huang, R. B.; Zheng, L. S.; Tao, J. A boracite metal-organic framework displaying selective gas sorption and guest-dependent spin-crossover behavior. *Chem. Commun*., **2013**, *49*, 10730.

[17] B. F. Hoskins and R. Robson, Infinite polymeric frameworks consisting of three dimensionally linked rod-like segments. *J. Am. Chem. Soc*., **1989**, *111*, 5962.

[18] In the same crystallization tube where **1** is obtained a different structure was also isolated (**1′**). The lattice parameters are: a = 24.5642(18) Å, b = 8.5680(8) Å, c = 29.493(2) Å, β = 98.956(6)°; V = 6132 Å^3. The crystal was very small not allowing a data quality for depositing the structure in the CCDC. However, we believe it is important to mention it. The new phase forms 1D chains composed of four TPB ligands and four $ZnCl_2$. The chains pack along the *b*-crystallographic direction and the overall structure is porous with 32 % of void space filled with solvent.

[19] The single crystal X-ray data was recorded at the B13-XALOC Macromolecular Crystallography beamline, Alba synchrotron, Barcelona, Spain. The structure of **1** is isostructural to that reported by Dehnen et al. (reference 14). However, we note two important differences: the framework does not show any disordered atom and six templating nitrobenzene molecules have been located crystallographically.

[20] For other icosahedron nanocage: Bilbesi, R. A.; Ronson, T. K.; Nitschke, J. R. A self-assembled $[Fe^{II}_{12}L_{12}]$ capsule with an icosahedral framework. *Angew. Chem. Int. Ed.*, **2013**, *52*, 9027-9030.

[21] The voids have been calculated using a spherical probe with a radius of 1.2 Å. L. J. Barbour. *Chem. Commun*., **2006**, 1163.

[22] Kawano, M.; Haneda, T.; Hashizume, D.; Izumi, F.; Fujita, M. A selective instant synthesis of a coordination network and its *ab initio* powder structure determination. *Angew. Chem. Int. Ed*., **2008**, *47*,1269-1271.

[23] Martí-Rujas, J.; Kawano, M.; Kinetic products in porous coordination networks: *ab initio* X-ray powder diffraction analysis. *Acc. Chem. Res.* **2013**, *46* 493-505.

[24] Martí-Rujas, J.; Islam, N.; Hashizume, D.; Izumi, F.; Fujita, M.; Song, H. J.; Choi, H. C.; Kawano, M. *Angew. Chem. Int. Ed*. **2011**, *50*, 6105–6108.

[25] The LeBail refinements were carried out using the GSAS (General Structure Analysis System) program: A. C. Larson and R. B. Von Dreele, GSAS, Los Alamos Laboratory Report No. LA-UR-86-748, 1987.

[26] Wu, Q.; Rauscher, P. M.; Lang, X.; Wojtecki, R. L.; de Pablo, J. J.; Hore, M. J. A.; Rowan, S. J. Poly[*n*]catenanes: Synthesis of molecular interlocked chains. *Science*, **2017**, *358*, 1434-1439.

[27] Grimme, S. Semiempirical hybrid density functional with perturbative second-order correlation. *J. Chem. Phys.*, **2006**, *124*, 34108.

[28] Famulari, A.; Raos, G.; Baggioli, A.; Casalegno, M.; Po, R.; Meille, S. V. A Solid State Density Functional Study of Crystalline Thiophene-Based Oligomers and Polymers. *J. Phys. Chem. B* **2012**, *116*, 14504−14509.

[29] Nicolini, T.; Famulari, A.; Gatti, T.; Martí-Rujas, J.; Villafiorita-Monteleone, F.; Canesi, E.; Meinardi, F.; Botta, C.: Parisini, E.; Meille, S.V.; Bertarelli C. Structure–Photoluminescence Correlation for Two Crystalline Polymorphs of a Thiophene–Phenylene Co-Oligomer with Bulky Terminal Substituents *J. Phys. Chem. Lett*, **2014**, *5*, 2171-2176.

[30] Catalano, L.; Karothu, D.; Schramm, S.; Ahmed, E.; Rezgui, R.; Barber, T.; Famulari, A.; Naumov, P. Dual-Mode Light Transduction through a Plastically Bendable Organic Crystal as an Optical Waveguide *Angew. Chem. Int. Ed*. **2018**, *57*, 17254-17258.

[31] Li, H.-T.; Guo, F.; Kou, M.; Famulari, A. Fu, Q.; Martí-Rujas, J. Gas–solid chemisorption/adsorption and mechanochemical selectivity in dynamic nonporous hybrid metal organic materials. *Inorg. Chem.*, **2017**, *56*, 6584-6590.

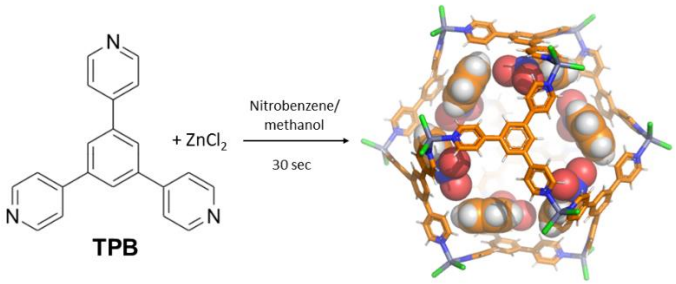

TOC